Some considerations about stress-relaxation in bending when an internal stress is present

F. POVOLO
Comisión Nacional de Energía Atómica, Dto. de Materiales, Av. del Libertador 8250, 1429 Buenos Aires, Argentina and Departamento de Física, Facultad de Ciencias Exactas y Naturales, Universidad de Buenos Aires, Pabellón 1, Ciudad Universitaria, 1428 Buenos Aires, Argentina

R. J. TINIVELLA, G. B. BOTTERI
Universidad Tecnológica Nacional, Facultad Regional San Nicolás, CC 118, 2900 San Nicolás, Argentina

Stress-relaxation in bending data, when the constitutive equation that describes the creep behaviour of the material includes an internal stress, are simulated numerically for two creep laws normally used in the literature. The simulation shows that the equations used to convert bending data to uniaxial conditions are also applicable when the internal stress changes with the applied stress.

1. Introduction

Stress-relaxation measurements in bending can give useful information on the creep behaviour of metals and alloys, particularly under critical conditions as, for example, under irradiation [1–5]. These experiments are much easier to perform than normal creep testing since several specimens can be tested at the same time to study the influence of a large number of variables (composition, thermo-mechanical treatment, etc.) simultaneously. In addition, the data can be obtained up to times of the order of those reached in creep, which is not possible in the case of stress-relaxation testing under uniaxial conditions. The analysis of bending data, however, is very complicated due to the fact that the specimens are subjected to a stress distribution.

In practice, flat specimens are located into holders with different radii, which give different maximum outer fibre stresses under elastic bending. The holders with the specimens are inserted into a furnace at the desired temperature, and removed periodically for curvature measurements. The radii of curvature R_i after releasing the specimens from the holders are normally determined by measuring the coordinates of different points with respect to a reference plane in the arc of circumference determined by the curved beam, and feeding the data to a computer program which calculates the average radius by a least-square fitting. In summary, the experiment provides the quantity

$$\sigma_b = \frac{Eh}{2}\left(\frac{1}{R_i} - \frac{1}{R}\right) \quad (1)$$

as a function of time. σ_b is the measured stress change at the surface of the bent specimen after releasing it from the holder, h is the thickness of the specimen, R is the radius of curvature of the holder and E is Young's modulus.

The initial stress Σ at the surface of the bent specimen is given by

$$\Sigma = Eh/2R \quad (2)$$

The fundamental problem of bending experiments is then to obtain information on the stress-relaxation behaviour of the material from the measured σ_b against $\log t$ curves, where t is the time, measured at different Σ values and at various temperatures. The analysis of the results is particularly complicated when the creep rate does not change linearly with the applied stress. Lewthwaite and Mosedale [6, 7] have analysed the stress-relaxation behaviour of beam and torsion specimens by assuming a law appropriate for irradiation creep. Povolo [8] solved the resulting mathematical expressions and gave a procedure to obtain the creep parameters from the stress-relaxation data. All these treatments assume a given creep law for the material and analyse the problem of obtaining the parameters of the particular creep law from the σ_b against $\log t$ curves. In other words, the stress-relaxation in bending data were considered in a stress against time diagram.

Povolo and Toscano [9, 10] have studied the problem of obtaining information on the creep behaviour of the material from the measured σ_b against $\log t$, independently from the creep law. The procedure used is based on the momentum, M, equilibrium equation for a rectangular beam of width b stressed in a circular holder, given

$$M = b\int_{-h/2}^{h/2} \sigma_r r\,dr = \frac{1}{6}\sigma_b b h^2 \quad (3)$$

where σ_r is the stress in a fibre at a distance r from the neutral axis, at any time t. The integral equation expressed by Equation 3 can be written in a differential form [9] and under the assumption that the

0022–2461

thickness of the specimen is constant, results in

$$\sigma_s = \sigma_r\left(\frac{h}{2}\right) = \frac{2}{3}\sigma_b + \frac{\Sigma}{3}\left(\frac{d\sigma_b}{d\Sigma}\right) \quad (4)$$

This equation shows that the stress at the surface of the beam, σ_s, before unloading, can be obtained from the measured quantity σ_b. The stress-relaxation data in bending can then be reduced to uniaxial conditions, i.e. to σ_s against t curves, by making measurements of σ_b against t with holders of different radii.

Another possibility appears when the radius of the holder is constant and the thickness of the specimens is variable. Equation 4 transforms in this case to

$$\sigma_s = \frac{2}{3}\sigma_b + \frac{h}{3}\left(\frac{d\sigma_b}{dh}\right) \quad (5)$$

showing that σ_s can be obtained from measurements of σ_b for different thicknesses, avoiding the use of different holders.

Equation 5 has been checked experimentally in specimens of Zircaloy-4[10] and Equation 4 has been used in zirconium alloys [9, 11–15], in stainless steel [16, 17] and in Inconel 718 [18] to convert stress-relaxation in bending data to uniaxial conditions. The problem with Equations 4 and 5, however, is that they were obtained from Equation 3 by using Leibniz's rule for differentiation of an integral dependent on a parameter, which requires the continuity of the derivative of the integrand [19]. This would not be the case, for example, when the creep law used includes an internal stress, which is reached at some points in the bent specimen. In fact, in uniaxial conditions the internal stress is only a limit for the applied stress when t tends to infinity.

It is the purpose of this paper to show that Equation 4 also gives reliable results when the creep or stress-relaxation law involves an internal stress, by using numerical simulation with typical expressions reported in the literature for creep or stress-relaxation behaviour.

2. Theoretical background

Equation 4 is applied to the experimental σ_b against $\log t$ curves, measured at different initial stresses Σ, on replacing the differential by small and finite increments, that is $d\sigma_b/d\Sigma \simeq \Delta\sigma_b/\Delta\Sigma$ at any time. Then, the numerical simulation will be performed according to the following procedure:

(i) A given constitutive equation for stress relaxation is assumed, that is, the law

$$\dot{\sigma} = f(\sigma^*) \quad (6)$$

is known. The dot indicates a derivative with respect to the time and $\sigma^* = \sigma - \sigma_i$ is the effective stress.

(ii) It is assumed that the specimen is bent elastically at the beginning of the experiment, so that the stress distribution is

$$\Sigma_r = 2\Sigma/hr \quad (7)$$

It is also assumed that the mechanism of creep is the same in tension as in compression, that the neutral axis remains at the centre of the beam and that the law $\sigma_i = \sigma_i(\Sigma)$ is known. Equation 1 is then integrated to give

$$\sigma = \sigma(t, \Sigma) \quad (8)$$

(iii) Once $\sigma(t, \Sigma)$ is known, Equation 3 written in the form

$$\sigma_b = \frac{6}{h^2}\int_{-h/2}^{h/2} \sigma_r r\, dr \quad (9)$$

is integrated analytically or numerically, leading to

$$\sigma_b = \sigma_b(t, \Sigma) \quad (10)$$

Furthermore, if Equation 10 is evaluated for two slightly different initial stresses at the surface, Σ_1 and Σ_2, given σ_{b1} and σ_{b2}, Equation 4 can be written as

$$\sigma_s(t, \bar{\Sigma}) = \frac{2}{3}\sigma_b + \frac{\bar{\Sigma}}{3}\left(\frac{\Delta\sigma_b}{\Delta\Sigma}\right) \quad (11)$$

where $\bar{\Sigma} = (\Sigma_1 + \Sigma_2)/2$, $\bar{\sigma}_b = (\sigma_{b1} + \sigma_{b2})/2$, $\Delta\sigma_b = \sigma_{b2} - \sigma_{b1}$ and $\Delta\Sigma = \Sigma_2 - \Sigma_1$.

The values given by Equation 11 can be compared with those given by Equation 8 for $\Sigma = \bar{\Sigma}$. This comparison will show whether Equation 11, used to convert bending data to uniaxial conditions, is also valid when an internal stress is present. The procedure just described will be applied to two constitutive equations which are commonly used in the literature, namely the Johnston–Gilman [20] and Kuznetsov–Pavlov [21] equations.

2.1. The Johnston–Gilman equation

In this model, the creep rate is given by

$$\dot{\varepsilon} = \phi\rho\boldsymbol{b}v_0\,(\bar{\sigma}/\sigma_0)^{m*} = \dot{\varepsilon}_0(\sigma - \sigma_i)^{m*} \quad (12)$$

with

$$\dot{\varepsilon}_0 = \phi\rho\boldsymbol{b}v_0/\sigma_0^{m*} \quad (13)$$

where ϕ is an orientation factor, ρ is the mobile dislocation density, $\boldsymbol{b}$ is the Burgers vector and v_0, σ_0 and m^* are material constants. For stress relaxation experiments

$$\dot{\varepsilon} = -\dot{\sigma}/E \quad (14)$$

where E is Young's modulus. Combining Equations 12 and 13 leads to

$$d\sigma/(\sigma - \sigma_i)^{m^*} = -\dot{\varepsilon}_0 E dt \quad (15)$$

which, integrated between Σ_r and σ, and 0 and t, gives

$$\sigma = \sigma_i + [(\Sigma_r - \sigma_i)^{(1-m^*)} - \dot{\varepsilon}_0 Et(1 - m^*)]^{1/(1-m^*)} \quad (16)$$

On introducing $x = 2r/h$ and taking into account Equation 7, Equation 16 can be written as

$$\sigma(x, t) = \sigma_i + [(\Sigma x - \sigma_i)^{(1-m^*)} - \dot{\varepsilon}_0 Et(1 - m^*)]^{1/(1-m^*)} \quad (17)$$

Moreover, Equation 9 is reduced in this case to

$$\sigma_b(x, t) = 3\int_0^1 \sigma(x, t)\, x\, dx \quad (18)$$

with $\sigma(x, t)$ given by Equation 17. Finally, the value of the integral in Equation 18 depends on the functional dependence of σ_i on Σ.

2.2. The Kuznetsov–Pavlov equation

In this case the creep rate is expressed by

$$\dot{\varepsilon} = \phi\rho b v_0 \sinh[C(\sigma - \sigma_i)] = \dot{\varepsilon}_1 \sinh[C(\sigma - \sigma_i)] \quad (19)$$

where C is a material constant. For stress relaxation, Equation 19 can be written as

$$d\sigma/\sinh[C(\sigma - \sigma_i)] = -E\dot{\varepsilon}_1 dt \quad (20)$$

which, integrated between Σ_r and σ, and 0 and t, and rearranging terms gives

$$\sigma(x, t) = \sigma_i - \frac{1}{C}\ln\left(\frac{e^{C(\Sigma x - \sigma_i)}(1 + e^{At}) + (1 - e^{At})}{e^{C(\Sigma x - \sigma_i)}(1 - e^{At}) + (1 + e^{At})}\right) \quad (21)$$

with

$$A = E\dot{\varepsilon}_1 C \quad (22)$$

3. Results

The expressions for $\sigma(x, t)$ and $\sigma_b(x, t)$ described in the preceding paragraph will be evaluated for different dependencies of σ_i on Σ. The different situations considered, some of which are illustrated in Fig. 1, are as follows:

(i) σ_i = constant, i.e. independent of Σ.

(ii) A linear variation of σ_i with Σ, i.e.

$$\sigma_i = \alpha\Sigma_r = \alpha x\Sigma \quad (23)$$

with three different values for the slope α, as indicated by the straight lines (a), (b) and (d) of Fig. 1. The full squares of the same figure show the dependence of σ_i on Σ obtained experimentally from stress relaxation in bending of stainless steel type AISI 304 at 773 K [16]. Moreover, the broken straight line corresponds to $\alpha = 0.027$ and the crosses indicate some experimental data for stress relaxation in bending of stainless steel type AISI 304 at 823 K [17].

(iii) A law of the type

$$\sigma_i = 55\{1 + \tanh[0.06(\Sigma_r - 85.71)]\} \quad \text{MPa} \quad (24)$$

as illustrated by curve (c) of Fig. 1. In this example, σ_i increases at first with Σ_r and then reaches a saturation value.

(iv) Curve (e) of Fig. 1 represents a dependence of σ_i on Σ_r of the form

$$\sigma_i = 25[1 + \tanh[0.03(\Sigma_r - 266)]\} \quad \text{MPa} \quad (25)$$

(v) Finally, the last situation that will be considered involves the case in which the internal stress increases during the relaxation due to "work-hardening" [22], i.e.

$$\delta\sigma_i = \theta\delta\varepsilon_p \quad (26)$$

where $\delta\varepsilon_p$ is the increment in plastic strain and θ is the work-hardening coefficient, which is assumed to be constant, i.e. workhardening increases linearly with the plastic strain. Moreover, since $\dot{\varepsilon}_p = -\dot{\sigma}/E$ for stress relaxation, Equation 26 can be written as

$$\delta\sigma_i(t) = \frac{\theta}{E}\delta\sigma(t) \quad (27)$$

where $\delta\sigma(t) = \sigma_0 - \sigma$, σ_0 being the stress at the beginning of relaxation ($t = 0$) and σ the stress at any instant t. In addition, on taking into account that

$$\sigma_i = \sigma_{i0} + \delta\sigma_i \quad (28)$$

where σ_{i0} is the internal stress at $t = 0$, combining Equations 27 and 28 gives

$$\sigma_i(t) = h - m\sigma(t) \quad (29)$$

with

$$h = \sigma_{i0} + \frac{\theta}{E}\sigma_0 \quad (30)$$

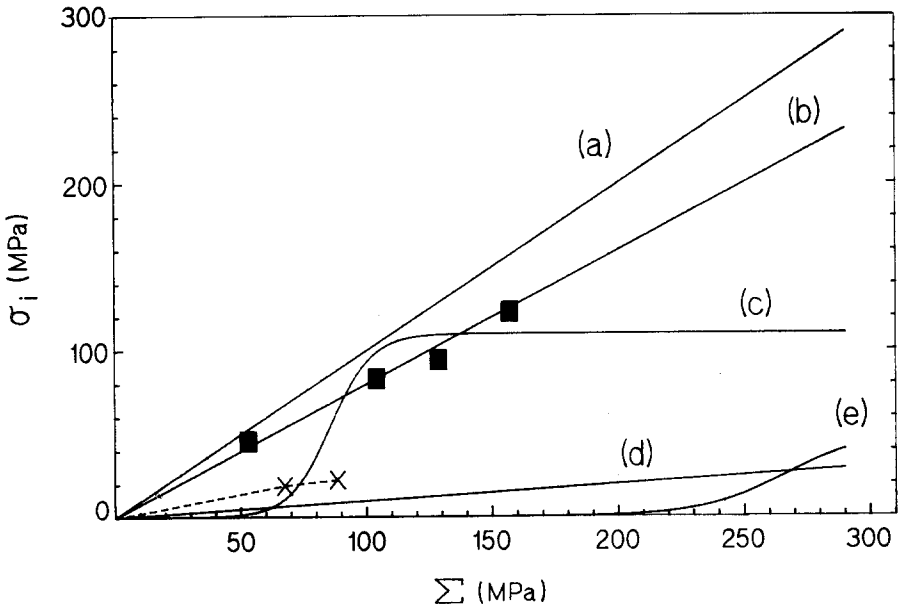

Figure 1 Dependence of the internal stress σ_i on the initial stress at the surface of the bent specimen, Σ, used for the calculation of the stress-relaxation curves: (a) $\alpha = 0.8$, (b) $\alpha = 0.4$, (c) $\sigma_i = 55\{1 + \tanh[0.06(\Sigma - 85.71)]\}$MPa, (d) $\alpha = 0.1$, (e) $\sigma_i = 25\{1 + \tanh[0.03(\Sigma - 266)]\}$ MPa. The broken curve corresponds to $\alpha = 0.027$. The full squares and the crosses indicate some experimental points obtained for stress-relaxation in bending in stainless steel AISI 304.

and

$$m = \theta/E \tag{31}$$

The different functional dependencies mentioned above will be used next to simulate, for the two constitutive equations mentioned above, the stress relaxation in bending. For σ_i = constant and $x = 1$, Equations 17 and 18 convert to

$$\sigma(\Sigma, t) = \sigma_i + [(\Sigma - \sigma_i)^{(1-m^*)} - \dot{\varepsilon}_0 E(1 - m^*)t]^{1/(1-m^*)} \tag{32}$$

and

$$\sigma_b(\Sigma, t) = (\sigma_i^3/\Sigma^2) + 3\int_{\sigma_i/\Sigma}^{1} \sigma(x, t)x\,dx \tag{33}$$

respectively, with $\sigma(x, t)$ given by Equation 17. Once the parameters σ_i, Σ, m^* and $\dot{\varepsilon}_0 E$ are given, Equation 32 allows a calculation of σ against t, for different values of Σ. Furthermore, on numerically integrating Equation 33 it is possible to evaluate σ_b against t for various values of Σ, and $\sigma_s(\bar{\Sigma}, t)$ by using Equation 11. The results obtained in this way, for three different values of Σ, are illustrated by curves A, B and C of Fig. 2 and the parameters used for the calculations are given in Table I. The broken curves represent σ_b and the full curves give $\sigma(\Sigma, t)$, as calculated with Equation 32, or $\sigma_s(\bar{\Sigma}, t)$ as calculated from σ_b by means of Equation 11. In effect, a perfect coincidence was obtained between $\sigma(\Sigma, t)$ and $\sigma_s(\bar{\Sigma}, t)$ for $\Sigma = \bar{\Sigma}$, indicating that Equation 4, used to convert bending data to uniaxial conditions, is valid for this case.

A similar procedure can be used for the constitutive equation represented by Equation 19. $\sigma(\Sigma, t)$ is calculated with Equation 21 for $x = 1$ for σ_i = constant; σ_b is obtained by numerically integrating Equation 33, with $\sigma(x, t)$ given by Equation 21, leading to $\sigma_s(\bar{\Sigma}, t)$ by means of Equation 11. Curves A*, B*, C* of Fig. 2, calculated with the parameters given in Table I, illustrate the results obtained for the same values of Σ as for curves A, B, C. Here also the broken curves indicate σ_b and the full ones either $\sigma(\Sigma, t)$ or $\sigma_s(\bar{\Sigma}, t)$ for $\bar{\Sigma} = \Sigma$. In summary, it can be stated that for the two constitutive equations represented by Equations 12 and 19. Equation 4 gives reliable results for uniaxial conditions when σ_i = constant.

It should be pointed out that the same notation will be used through all the curves that will follow, i.e. the curves with A, B, C and A*, B*, C* will indicate the results obtained with the Johnston–Gilman equation and the Kuznetsov–Pavlov equation, respectively. Furthermore, in each case the broken curves correspond to σ_b and the full ones to either $\sigma(\Sigma, t)$ or $\sigma_s(\bar{\Sigma}, t)$, since a perfect coincidence was always found between σ and σ_s.

The concepts developed can also be applied when σ_i changes linearly with Σ, i.e. when the internal stress is described by Equation 23. The Johnston–Gilman equation leads in this case to

$$\sigma(x, t) = \alpha\Sigma x + \{[(1 - \alpha)\Sigma x]^{(1-m^*)} - \dot{\varepsilon}_0 E(1 - m^*)t\}^{1/(1-m^*)} \tag{34}$$

which for $x = 1$ reduces to

$$\sigma(\Sigma, t) = \alpha\Sigma + \{[(1 - \alpha)\Sigma]^{(1-m^*)} - \dot{\varepsilon}_0 E(1 - m^*)t\}^{1/(1-m^*)} \tag{35}$$

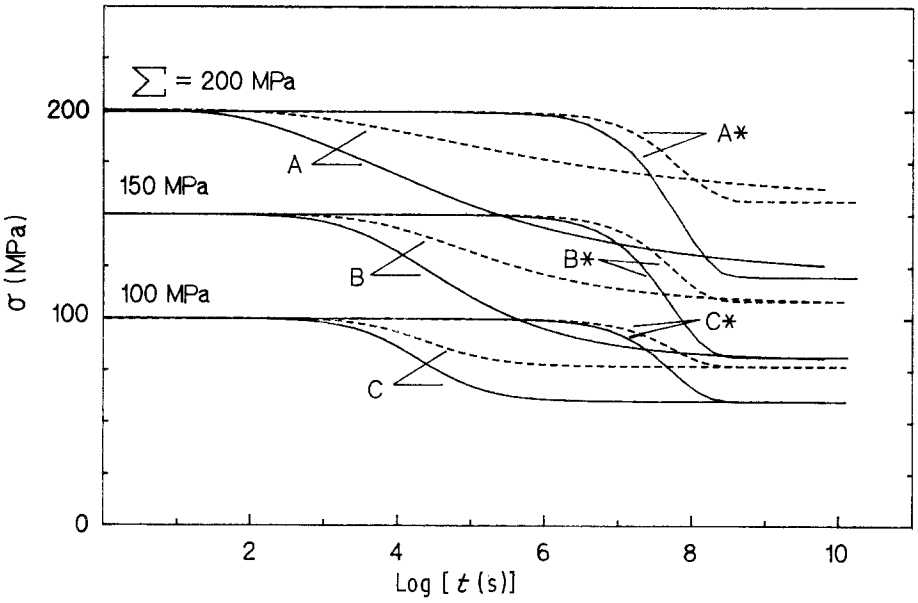

Figure 2 Stress-relaxation curves for σ_i = constant, calculated with the parameters given in Table I.

TABLE I Parameters used for calculation of the stress-relaxation curves for σ_i = constant, shown in Fig. 2; m^*, $\dot{\varepsilon}_0 E$ and $\dot{\varepsilon}_1 E$, C are for the Johnston–Gilman and Kuznetsov–Pavlov equation, respectively

Curve	Σ (MPa)	σ_i (MPa)	m^*	$\dot{\varepsilon}_0 E$ ($MPa^{(1-m^*)}s^{-1}$)	$\dot{\varepsilon}_1 E$ ($MPa\,s^{-1}$)	C (MPa^{-1})
A or A*	200	120	7	1×10^{-15}	1×10^{-6}	0.02
B or B*	150	80	4	1×10^{-10}	1×10^{-6}	0.02
C or C*	100	60	2	1×10^{-6}	1×10^{-6}	0.02

Moreover, once $\sigma(x, t)$ is known, σ_b can be calculated by numerically integrating Equation 18 and $\sigma_s(\bar{\Sigma}, t)$ can be obtained by using Equation 11. A similar procedure can be followed when the functional dependence of σ_i on Σ_r is represented by Equations 24 and 25, except that σ_i should be replaced by the appropriate expression in Equation 17. The detailed calculations are easy to perform and will not be presented in this paper. Finally, in the case where the constitutive equation is represented by Equation 19, the appropriate functional dependence $\sigma_i = \sigma_i(\Sigma)$ should be incorporated into Equation 21 and the calculations can be carried on as for the case of the Johnston–Gilman equation.

Fig. 3 shows the results obtained when the internal stress varies according to Equation 23 and the parameters used for the calculations take the values indicated in Table II. It is interesting to notice in this figure that for curve A*, $\sigma_b = \sigma = \sigma_s$ and for curves B* and C* only a slight difference is found between σ_b and σ or σ_s.

Curves A, A* and B, B* of Fig. 4 illustrate the stress

TABLE II Parameters used for calculation of the stress-relaxation curves when the internal stress changes according to Equation 23, shown in Fig. 3; for A*, B* and C*, $C = 0.02$ MPa and $\dot{\varepsilon}_1 E = 1 \times 10^{-6}$ MPa s^{-1}

Curve	Σ (MPa)	α	m^*	$\dot{\varepsilon}_0 E$ (MPa$^{(1-m^*)}$s^{-1})
A or A*	200	0.8	7	1×10^{-5}
B or B*	150	0.4	4	1×10^{-10}
C or C*	100	0.1	2	1×10^{-6}

TABLE III Parameters employed for calculation of the stress-relaxation curves of Fig. 4, where σ_i changes according to Equation 24 or 25; $\Sigma = 282$ MPa, $\dot{\varepsilon}_0 E = 1 \times 10^{-10}$ MPa$^{(1-m^*)}$s^{-1}, $\dot{\varepsilon}_1 E = 1 \times 10^{-6}$ MPa s^{-1}, $m^* = 4$ and $C = 0.02$ MPa^{-1}

Curve	σ_i (MPa)
A or A*	$25\{1 + \tanh[0.03(\Sigma - 266)]\}$
B or B*	$55\{1 + \tanh[0.06(\Sigma - 85.71)]\}$

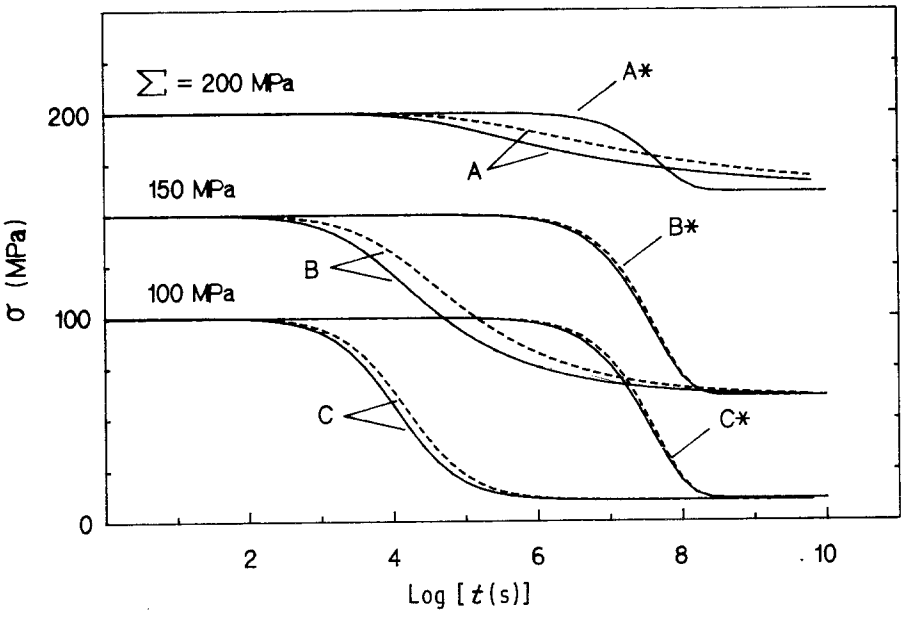

Figure 3 Stress-relaxation curves for $\sigma_i = \alpha\Sigma$, calculated with the parameters given in Table II.

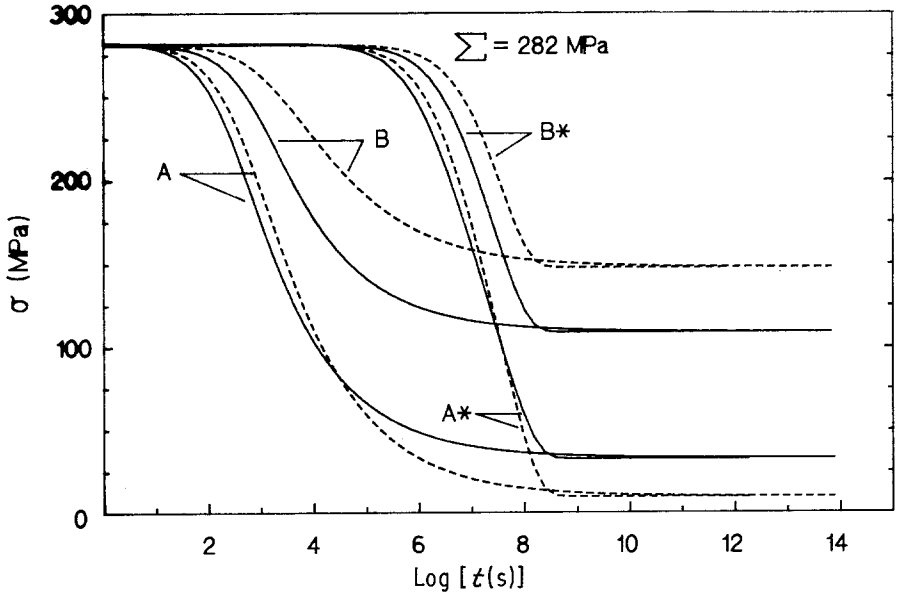

Figure 4 Stress-relaxation curves obtained when the internal stress changes according to Equations 24 or 25. The parameters used for the calculations are indicated in Table III.

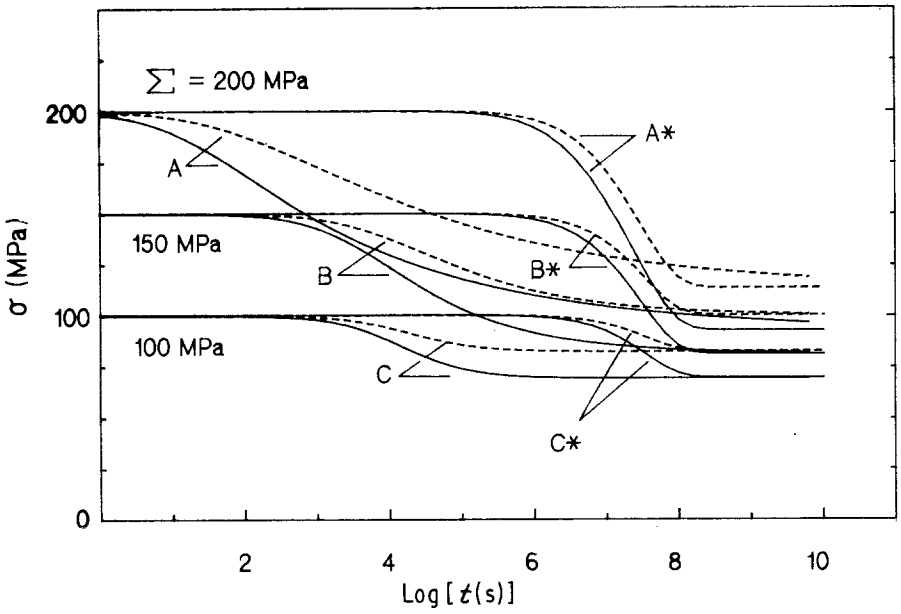

Figure 5 Stress-relaxation curves when work-hardening occurs during the relaxation, i.e. when the internal stress varies according to Equation 28. The parameters used for the calculations are indicated in Table IV.

TABLE IV Parameters used for the calculation of the stress-relaxation curves of Fig. 5, where work-hardening is present; $\sigma_{i0} = 50$ MPa, $\theta/E = 0.3$, $\dot{\varepsilon}_1 E = 1 \times 10^{-6}$ MPa s^{-1} and $C = 0.02$ MPa^{-1}

Curve	Σ (MPa)	$\dot{\varepsilon}_0 E$ (MPa$^{(1-m^*)}$ s^{-1})	m^*
A or A*	200	1×10^{-15}	7
B or B*	150	1×10^{-10}	4
C or C*	100	1×10^{-6}	2

relaxation behaviour when the internal stress changes according to Equations 25 and 24, respectively. These curves were evaluated for $\Sigma = 282$ MPa, with the parameters given in Table III.

Finally, the situation in which strain-hardening occurs during relaxation will be considered. The Johnston–Gilman model, for example, on substituting Equation 29 into Equation 23 and integrating, taking into account that $\sigma_0 = \Sigma x$, gives

$$\sigma(x, t) = \frac{1}{1 + \tilde{\theta}} \left\{ \sigma_{i0} + \tilde{\theta}\Sigma x + \left[\frac{(1 + \theta)}{n} \dot{\varepsilon}_0 E t + (\Sigma x - \sigma_{i0})^{-1/n} \right]^{-n} \right\} \quad (36)$$

where

$$\tilde{\theta} = \theta/E \quad (37)$$

and

$$n = 1/(m^* - 1) \quad (38)$$

On assuming that σ_{i0} is independent of the initial state of loading, Equation 33, with σ_i substituted by σ_{i0} and $\sigma(x, t)$ given by Equation 36, can be used to calculate σ_b. Similar considerations can be made for the Kuznetsov–Pavlov equation. The results obtained in this way are illustrated in Fig. 5, for $\theta/E = 0.3$ and $\sigma_{i0} = 50$ MPa. The parameters used for the calculations are given in Table IV.

4. Discussion and conclusions

The examples considered in the paper show that, even in the case where an internal stress is present in the constitutive equation that describes the stress-relaxation behaviour of the material, Equation 4 gives reliable results when converting bending data to uniaxial conditions. It should be pointed out that the values for the different parameters used to calculate the stress-relaxation curves of Figs 2 to 5 are in the range of those encountered in actual experimental data for stress-relaxation in bending in different alloys [9–17].

It is important to mention that the most detailed bending experiments were performed in zirconium alloys, since the results were correlated with creep and load-relaxation experiments. In fact, the bending data obtained in specimens under different thermo-mechanical conditions, once converted to uniaxial conditions, could be described by the same constitutive equation used in creep and load-relaxation [12–15]. Furthermore, meaningful physical parameters could be obtained from the experimental curves since they could be described by a physical model involving the effects of jog–drag upon the rate of creep in a material containing a three-dimensional dislocation network. In this context, a correlation was established between the initial stress, Σ, and the ratio of cell diameter to mean dislocation spacing [12, 14, 15]. The constitutive creep equation used, however, did not include an internal stress.

Bending data in stainless steel were interpreted in terms of a constitutive equation including an internal stress, such as Equation 12 [16, 17]. After reduction of the data to uniaxial conditions, the dependence of the internal stress on the initial stress, i.e. the law $\sigma_i = \sigma_i(\Sigma)$, was obtained directly from the experimental curves. This was also the case when the internal stress, in addition, varied with the applied stress. The stress-relaxation curves simulated in this paper and shown in Figs 2 to 5 confirm the procedure used since Equation 4, employed for the reduction of the bending data to uniaxial conditions, is applicable also

when $\sigma_i \neq 0$. In summary, it can be concluded that stress-relaxation data in bending can also give reliable information on the creep law for the material in the presence of an internal stress.

Acknowledgements

This work was supported in part by the Consejo Nacional de Investigaciones Científicas y Tecnicas (CONICET) and the "Proyecto Multinacional de Materiales" AOS-CNEA.

References

1. P. H. KREYNS and M. W. BURKART, *J. Nucl. Mater.* **26** (1968) 87.
2. R. A. WOLFE and B. Z. HYATT, *ibid.* **45** (1972/73) 181.
3. D. E. FRASER, P. A. ROSS-ROSS and A. R. CAUSEY, *ibid.* **46** (1973) 281.
4. A. R. CAUSEY, *ibid.* **54** (1974) 64.
5. G. L. WIRE and J. L. STRAALSUND, *ibid.* **64** (1977) 254.
6. G. W. LEWTHWAITE and D. MOSEDALE, *Br. J. Appl. Phys.* **17** (1966) 821.
7. *Idem., J. Nucl. Mater.* **31** (1969) 226.
8. F. POVOLO, *ibid.* **68** (1977) 308.
9. F. POVOLO and E. H. TOSCANO, *ibid.* **74** (1978) 76.
10. *Idem., ibid.* **78** (1978) 217.
11. F. POVOLO and M. HIGA, *ibid.* **91** (1980) 189.
12. F. POVOLO and P. N. PESZKIN, *Res. Mechanica* **6** (1983) 233.
13. F. POVOLO and A. J. MARZOCCA, *J. Nucl. Mater.* **98** (1981) 322.
14. F. POVOLO and J. C. CAPITANI, *J. Mater. Sci.* **19** (1984) 2969.
15. F. POVOLO, A. J. MARZOCCA and J. C. CAPITANI, *Phil. Mag.* **A48** (1983) 759.
16. F. POVOLO and R. J. TINIVELLA, *J. Mater. Sci.* **19** (1984) 1851.
17. F. POVOLO, R. J. TINIVELLA, J. F. REGGIARDO and G. B. BOTTERI, *J. Mater. Sci.* **27** (1992) 1505.
18. F. POVOLO and J. F. REGGIARDO, *J. Mater. Sci.* **23** (1988) 241.
19. B. M. BUDAK and S. V. FOMIN, "Multiple Integrals, Field Theory and Series" (MIR, Moscow, 1973) Ch. 10.
20. W. G. JOHNSTON and J. J. GILMAN, *J. Appl. Phys.* **30** (1959) 139.
21. R. I. KUZNETSOV and V. A. PAVLOV, *Fiz. Metallov i Metallovedenie* **25** (1968) 934.
22. V. I. DOTSENKO, *Phys. Status Solidi (b)* **93** (1979) 11.

Received 8 July 1991
and accepted 17 July 1992